Carbohydrate Research, 170 (1987) 1–17
Elsevier Science Publishers B.V., Amsterdam – Printed in The Netherlands

ASSIGNMENTS OF THE ^{1}H- AND ^{13}C-N.M.R. SPECTRA OF TOBRAMYCIN AT LOW AND HIGH pH

LÁSZLÓ SZILÁGYI
Department of Organic Chemistry, Lajos Kossuth University, P.O.B. 20, H-4010 Debrecen (Hungary)
(Received February 20th, 1987; accepted for publication, May 15th, 1987)

ABSTRACT

The ^{1}H-n.m.r. spectra (200 MHz) of protonated (pD 3.9) and non-protonated (pD 11.9) tobramycin have been analysed completely by 2D methods. The $^3J_{H,H}$ values are consistent with an essentially undistorted $^4C_1$ conformation for each of the three moieties and are practically independent of the state of protonation. The resonances in the ^{13}C-n.m.r. spectrum (50 MHz) have been reassigned at both pD values on the basis of 2D ^{1}H–^{13}C chemical-shift correlation and 1D selective INEPT measurements.

INTRODUCTION

Tobramycin (**1**), an important member of the aminoglycoside family[1] of antibiotics, has been studied extensively by ^{13}C- and ^{15}N-n.m.r. methods[2–5], but the assignment of the ^{1}H resonances appears not to have been reported. The complete, *a priori* assignments[6] of the ^{1}H-n.m.r. spectra of solutions of tobramycin in D_2O at pD 3.9 and 11.9 (*i.e.*, under conditions where the five amino groups are either protonated or non-protonated, respectively) are now reported. The various versions of 2D homonuclear chemical-shift correlation spectroscopy[7] are powerful tools for assigning completely the ^{1}H-n.m.r. spectra of medium-sized oligosaccharides[8–10]. The double-quantum filtered, pure-phase, ^{1}H–^{1}H chemical-shift correlation (DQ-COSY)[11–12] and multiple-step homonuclear relayed-coherence-transfer (RCT)[13,14] techniques have been applied to tobramycin and the assignments confirmed by 1D homonuclear n.O.e. measurements[15] and spectrum simulation.

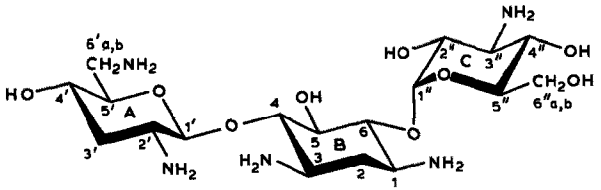

1

0008-6215/87/$ 03.50

An independent ^{13}C assignment has been deduced also on the basis of the proton chemical shifts through 2D ^{1}H–^{13}C chemical-shift correlation[16] and 1D selective INEPT[17] measurements. The results require some minor amendments to the early assignments of Wenkert *et al.*[2] based on empirical considerations and protonation shift data.

RESULTS AND DISCUSSION

The ^{1}H-n.m.r. spectrum of tobramycin is sensitive to the pH of the sample because of protonation of the amino groups. ^{13}C- (ref. 2) and ^{15}N-n.m.r.[5] studies showed that the amino groups in tobramycin are fully protonated at pH <5 and deprotonated at pH >10. Spectra have therefore been obtained for solutions in D_2O at pD 11.9 and 3.9.

^{1}H-N.m.r. data at pD 11.9. — The normal ^{1}H-n.m.r. spectrum and the pure absorption phase DQ-COSY map are shown in Figs. 1A and 2, respectively. The two doublets at 5.11 and 5.01 p.p.m. were assigned specifically to H-1′ and H-1″ in rings A and C, respectively, as follows. The former signal gives rise to a cross-peak with a resonance at 2.92 p.p.m. (omitted from Fig. 2 in order to allow a clearer representation of the other, more crowded region of the spectrum, but seen clearly in the double-RCT map in Fig. 3) which, in turn, shows correlations with the multiplets at 1.99 and 1.57 p.p.m. (cross-peaks 2′3′*e* and 2′3′*a* in Fig. 2). This sequence of *J*-connectivity unambigously assigns the doublet at 5.11 p.p.m. to H-1′ since the multiplet at 1.57 p.p.m. can be assigned only to the H-3′*a* resonance on the basis of its chemical shift. H-3′*a* has two further correlations with the signals at 1.99 and 3.48 p.p.m. The first one trivially originates from the geminal coupling with H-3′*e*, whereas the second pinpoints the chemical shift of the H-4′ resonance. The chain of *J*-coupling connectivity is broken here because the near-isochronous character of H-4′ and H-5′ (*vide infra*) results in a cross-multiplet which, complicated by strong coupling effects, is too near to the diagonal to be detected. However, this gap could be filled easily by observing the 3′*e*6′b and 3′*a*6′b correlations in the double-RCT map (Fig. 3) and it was then straightforward to trace down the coupling network through cross-peaks 6′a6′b, 5′6′a, and 5′6′b in the DQ-COSY map (Fig. 2) and to complete the assignments for ring A. From a comparison of the cross-peaks 3′*a*4′ and 5′6′a and/or 5′6′b, it is apparent that H-4′ and H-5′ are nearly isochronous; the "virtual coupling" effects[18] arising therefrom are clearly visible in the non-first-order appearance of the H-3′*a* multiplet (1.57 p.p.m., Fig. 1A) and, to a lesser extent, as distortions of lineshape in the H-6′b multiplet at 2.70 p.p.m. Several single-RCT cross-peaks are also present in Fig. 3 which have been identified in a separate single-RCT experiment (not shown). Only the correlations 1′3′*e* and 1′3′*a* need to be mentioned since they provide further support for assigning the anomeric doublet at 5.11 p.p.m. to H-1′.

Unambiguous assignment of the resonances of the 2-deoxystreptamine moiety (ring B) is complicated by the approximate symmetry of the molecule

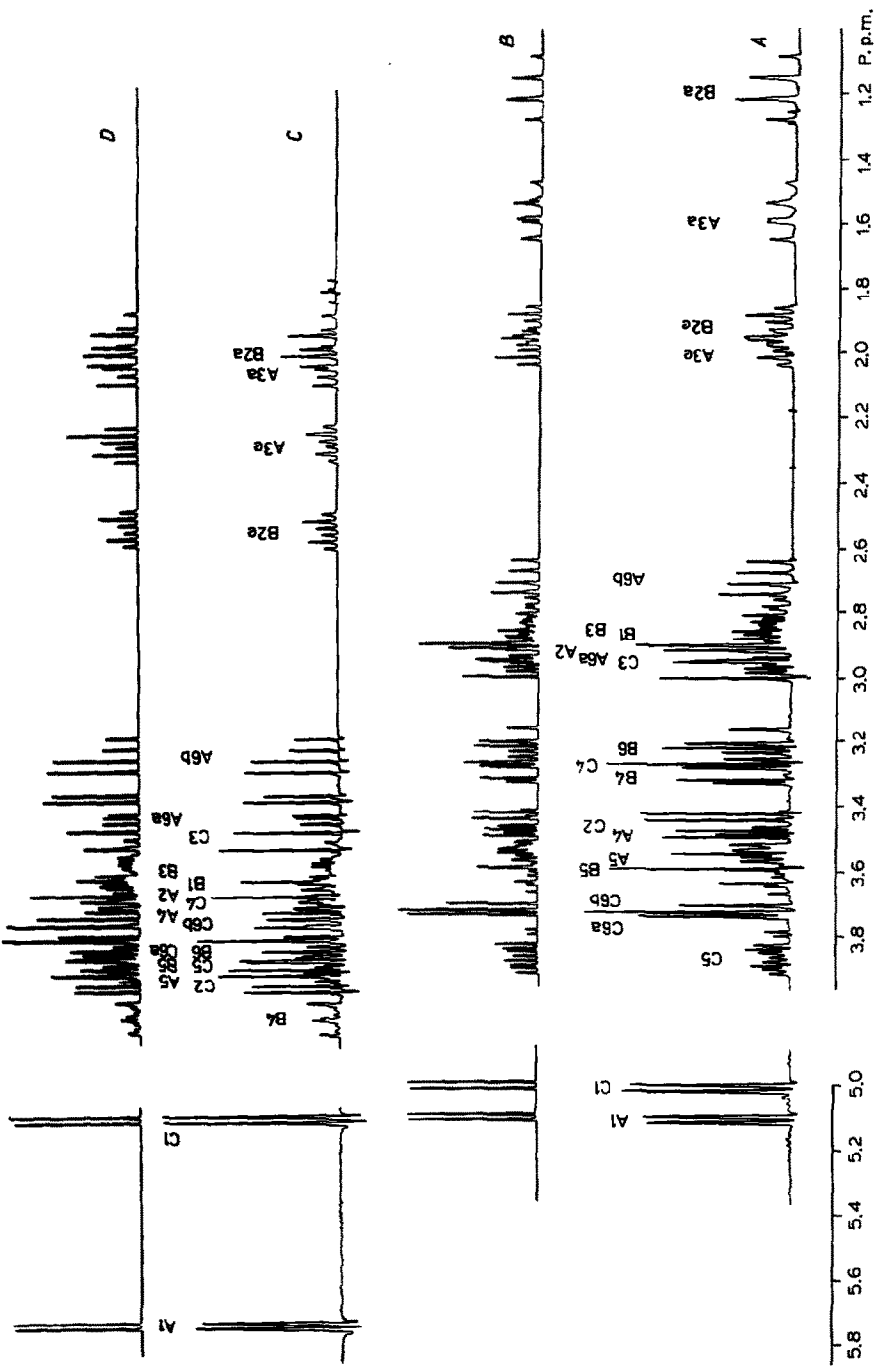

Fig. 1. Resolution-enhanced ^{1}H-n.m.r. spectra (200 MHz) of tobramycin recorded for solutions in D_2O at 40°: at pD 11.9, *A* measured and *B* calc.; at pD 3.9, *C* measured and *D* calc.

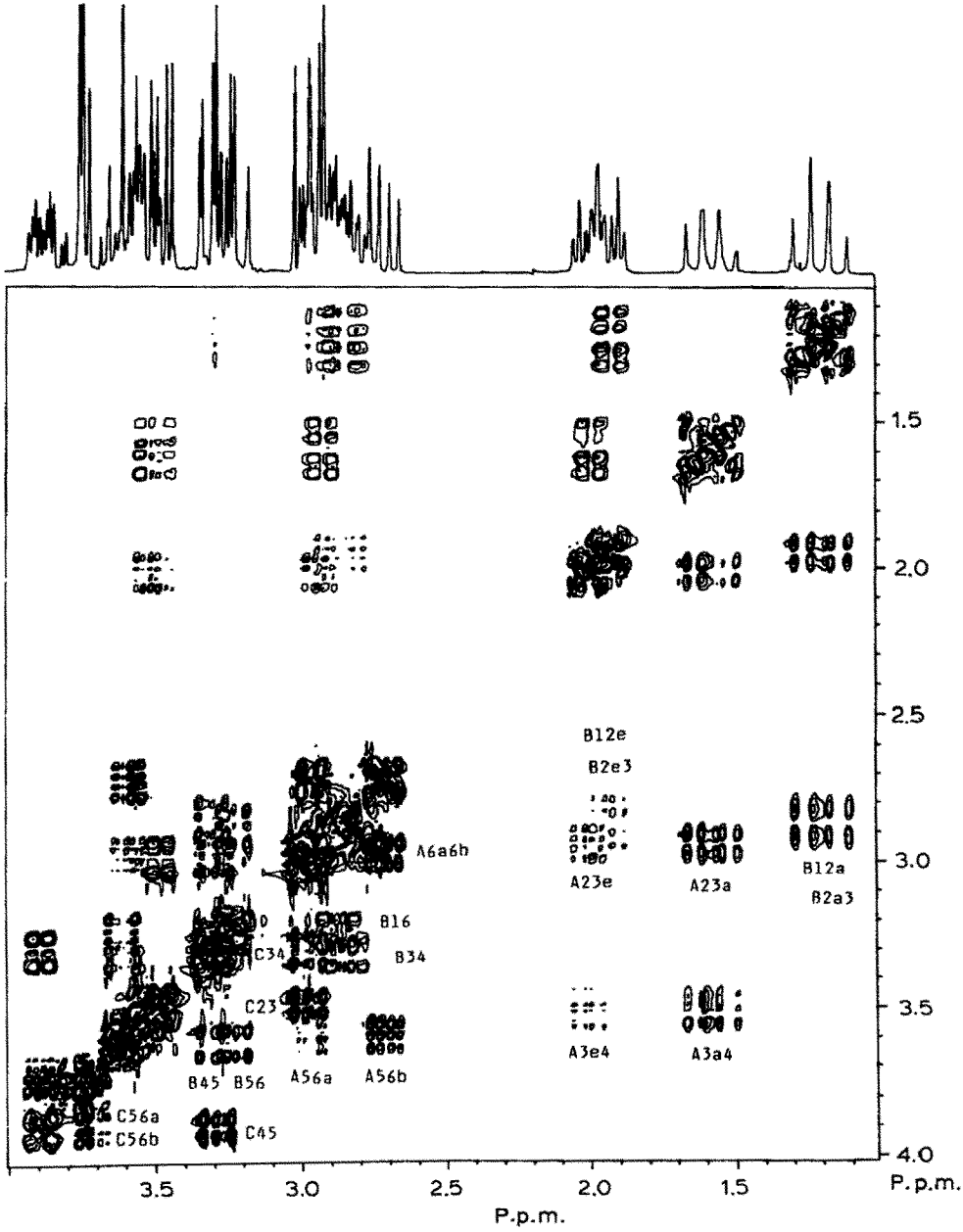

Fig. 2. Double-quantum filtered, pure absorption-phase COSY map displaying $^1H/^1H$-correlations between non-anomeric CH-protons of tobramycin at 40° and pD 11.9. The time-domain data matrix of 512 × 256 data points was multiplied in both t_1 and t_2 dimensions by sine-bell weighting functions shifted by $\pi/4$, zero-filled to 1K × 1K points and double Fourier-transformed to give a digital resolution of 1.7 Hz/data point in both the F_1 and F_2 dimensions. Positive and negative levels are plotted without distinction. Cross-peaks are labelled with reference to rings A–C; thus, A2*e*3 stands for the 2D multiplet revealing cross-correlation between H-2′*e* and H-3′, *etc.*

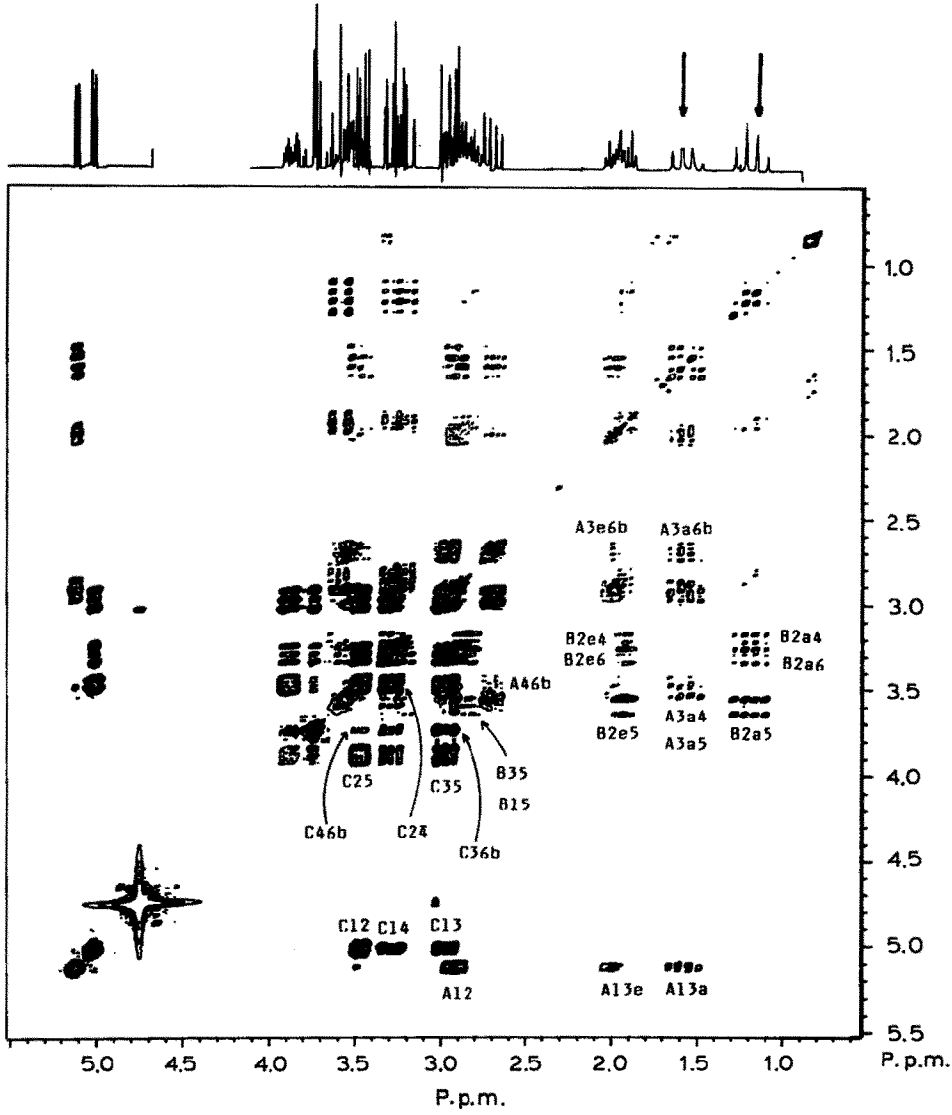

Fig. 3. Homonuclear, ^{1}H double-relay-coherence-transfer (RCT) 2D-map of tobramycin for a solution in D_2O at pD 11.9 at 40°. The delays for both relay periods were set to 60 ms; 64 transients were accumulated for each of the 256 t_1 increments, and sine-bell weighting functions were applied in both dimensions to the time-domain matrix prior to 2D Fourier-transformation. The data are shown in absolute value representation; other parameters are identical with those given in the legend to Fig. 2. The relevant COSY and single-relay cross-peaks are also labelled. The heavy arrows point to sites at which vertical cross-sections *A* and *B* shown in Fig. 5 were taken.

arising from the symmetrical disposition of rings A and C. The DQ-COSY map (Fig. 2) therefore provides little useful information for establishing the *J*-connectivity path in this part of the molecule. The resonances of H-2*e* and H-2*a*, trivially identified (by exclusion) at 1.92 and 1.19 p.p.m., respectively, give rise to cross-peaks with signals at 2.8–2.9 p.p.m. These cross-peaks consist of two overlapping 2D-multiplets evidently arising from couplings to H-1 and H-3. However, it is not possible to trace the *J*-connectivity beyond this point unles the latter two resonances are unambiguously distinguished. In following the *J*-connectivity path from the H-1/H-3 region of the diagonal (midpoints at 2.86 and 2.83 p.p.m.), two cross-peaks are found which locate H-4 and H-6 at 3.2–3.3 p.p.m. These multiplets partially overlap each other and also the 3″4″ cross-peak (*vide infra*) but, nevertheless, their connectivity can be traced down to H-5 at 3.59 p.p.m. This assignment was further confirmed by the observation of the 2*e*5 and 2*a*5 cross-peaks in the double-RCT map (Fig. 3). The ambiguity concerning the H-1/H-3 and H-4/H-6 assignments cannot be resolved by using connectivity considerations in ring B alone. On the other hand, knowing that ring B is glycosylated by nebrosamine (A) and kanosamine (C) moieties at positions 4 and 6, respectively, allows the specific assignments for H-4 and H-6 to be deduced by looking at the possibility of detecting interannular $^1H/^1H$ n.O.e. between H-1′ and H-4 and/or H-1″ and H-6. Such effects in oligosaccharides[19,20] are useful for establishing the sequence of the constituent units[8,21]. Fig. 4A shows that irradiation at the position (5.11 p.p.m.) of the anomeric doublet for H-1′ causes considerable enhancements in the intensities of the H-2′ multiplet (16%) and of a triplet at 3.29 p.p.m. (15%). The latter should arise from an H-1′/H-4 dipolar interaction and thereby identifies H-4. On the other hand, irradiation at the position (5.01 p.p.m.) of the H-1″ resonance results in a 17% enhancement of the H-6 resonance at 3.21 p.p.m., in addition to an 18% enhancement of that of H-2″ at 3.46 p.p.m. (*vide infra*; Fig. 4B). The specific assignments for H-1 and H-3, by way of the cross-peaks 16 and 34, respectively, observed in the DQ-COSY map (Fig. 2), are now straightforward.

The *J*-coupling connectivity in ring C could be readily established from H-1″ to H-5″ by identifying the relevant cross-peaks in the DQ-COSY map (Fig. 2). The partial overlap, mentioned above, of cross-peak 3″4″ with cross-peaks 16 and 34 of ring B did not seriously interfere with this assignment. Although the correlation 6″a6″b could not be observed in the DQ-COSY map (Fig. 2), presumably because of strong coupling, abundant cross-check possibilities were provided by the single- (not shown) and double-RCT (Fig. 3) maps. The correlation peaks identified in these spectra are collected in Table I. A triple-RCT experiment was also performed at pD 11.9, but the only cross-peak identified as one arising from a triple-RCT process was that between H-1″ and H-5″. Since lower-order RCT and COSY correlations are also present in this map (not shown), a cross-section parallel to the F_2 axis taken at the "height" of the H-1″ chemical shift value amounts to a partial "sub-spectrum" of residue C from H-1″ to H-5″ (Fig. 5). Complete "sub-spectra" for residues A and B can, in principle, be extracted from the *double*-RCT map by

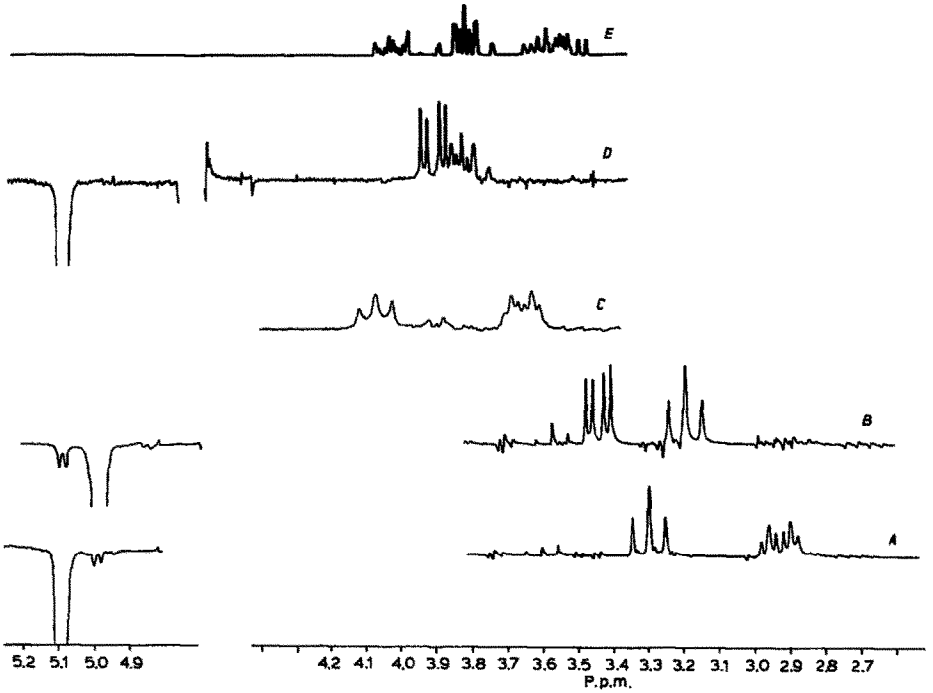

Fig. 4. Homonuclear, ^{1}H difference n.O.e. spectra of tobramycin measured for solutions in D_2O at 40°, showing the effects of pre-irradiation of H-1′ at pD 11.9 (*A*) and pD 3.9 (*C*), and of H-1″ at pD 11.9 (*B*) and pD 3.9 (*D*), and a calculated sub-spectrum for residue B for the conditions prevailing at pD 3.9 (*E*).

taking cross-sections at the chemical shift values of H-3′*a* and H-2*a* (indicated by arrows in Fig. 3), respectively. However, due to extensive cancellation effects[14], the cross-sections are not expected to reproduce faithfully the appropriate sub-spectra (see Fig. 5).

^{1}H-N.m.r. data at pD 3.9. — Protonation of all five amino groups of tobramycin is practically complete at this pH. Accordingly, no change was observed in the ^{1}H-n.m.r. spectrum on going from pD 3.9 to 1.0. On the other hand, there are substantial differences between the spectra recorded for solutions at pD 3.9 and 11.9 (Fig. 1). The most conspicuous changes are connected with large increases in the chemical shifts of the resonances for H-1′, H-3′*e*, H-3′*a*, H-2*e*, and H-2*a* upon protonation.

Extensive overlap and strong coupling effects (*vide infra*) in the ^{1}H-n.m.r. spectrum of the protonated form rendered analysis more difficult compared to that at high pD. The starting point of the assignment procedure was again the DQ-COSY spectrum, but the crowding of signals in the 1D spectrum also resulted in many overlaps among cross-multiplets in the 2D map. Beginning with the protons in ring A, the chemical shifts for the resonances of H-1′, H-3′*e*, and H-3′*a* were inferred without difficulty from a single-RCT experiment (not shown). It was then

TABLE I

^{1}H-N.M.R. DATA[a] (200 MHz) FOR TOBRAMYCIN IN D_2O

Proton	*pD 11.9*	*pD 3.9*	*Protonation shift*[b]	*Method of assignment*[c]
1′	5.11	5.76	0.65	R1(3′*e*), R1(3′*a*)
2′	2.92	3.67	0.75	C(3′*a*), C(1′), C(3′*e*), n.O.e. (1′)
3′*e*	1.99	2.29	0.30	$\delta, J_{2',3'e}$
3′*a*	1.57	2.02	0.45	$\delta, J_{3'a,4'}$
4′	3.48	3.72	0.24	R1(6′b), R1(6′a)[f]
5′	3.57	3.93	0.36	C(6′a), C(6′b), R1(3′*a*)[f]
6′a	2.94	3.41	0.47	C(6′b), R2(3*a*)[f]
6′b	2.70	3.26	0.56	R2(3′*e*), R2(3′*a*)
1	2.86	3.63	0.77	C(2*e*)[d], C(2*a*)[d], C(6)[d], R1(5)[d,e]
2*e*	1.92	2.55	0.63	$\delta, J_{1,2e}, J_{2e,3}$
2*a*	1.19	1.99	0.80	$\delta, J_{1,2a}, J_{2a,3}$
3	2.83	3.59	0.76	C(2*e*)[d], C(2*a*)[d,e], C(4), R1(5)[d,e]
4	3.29	4.07	0.78	R1(2*e*), R1(2*a*), n.O.e. (1′)
5	3.59	3.88	0.29	C(4)[d], C(6)[d,e], R2(2*e*)[e], R2(2*a*)[e]
6	3.21	3.83	0.62	R1(2*e*), R1(2*a*), n.O.e. (1″)
1″	5.01	5.12	0.11	δ
2″	3.46	3.95	0.49	C(1″), n.O.e. (1″)
3″	2.96	3.50	0.54	C(2″), R1(1″)
4″	3.27	3.69	0.42	C(3″), R1(2″)[e], R2(1″)
5″	3.87	3.90	0.03	C(4″)[e], R1(3″)[e], R2(2″)[e], R3(1″)[e]
6″a	3.75	3.84	0.09	C(5″)[e], R1(4″)[e], R2(3″)[e]
6″b	3.71	3.75	0.04	

[a]Internal sodium 4,4-dimethyl-4-silapentane-1-sulfonate for solutions in D_2O at 40°. [b]δ (pD 3.9) − δ (pD 11.9). [c]C, COSY; R1–R3, single, double, and triple RCT with the coupling partner in parentheses; n.O.e., 1D-homonuclear n.O.e. with the irradiated proton in parentheses, correlations were detected at both pD values if not stated otherwise. [d]See text for further explanation. [e]Not detected at pD 3.9. [f]Not detected at pD 11.9.

evident from the DQ-COSY map (not shown) that the resonances of H-2′ and H-4′ have very similar chemical shifts. Localisation of the H-5′ multiplet therefore was not possible in this map, but it could be identified, by way of the 3′*a*5′ relayed cross-peak, in the single-RCT map [the 3′*e*5′ cross-peak was extremely weak but could be seen readily in the double-RCT map (Fig. 6)]. The *J*-coupling connectivity could then be completed by identifying the 4′6′a, 4′6′b, and 5′6′a, 5′6′b cross-peaks in the single-RCT and DQ-COSY maps, respectively. These assignments were further corroborated by the appearance of the 3′*a*6′a, 3′*a*6′b, and 3′*e*6′b (and very weak 3′*e*6′a) cross-multiplets in the double-RCT map (Fig. 6). The "sub-spectrum" comprising the resonances of ring A, as extracted from the double-RCT map, is shown in Fig. 5.

The assignments of the resonances of the 2-deoxystreptamine moiety (ring B) could be achieved following the approach adopted at pD 11.9. The resonance for H-4 (or H-6) was readily identified by localising the single-RCT cross-peaks from H-2*e* and H-2*a* (four in all; namely, 2*e*4, 2*e*6, 2*a*4, and 2*a*6) in the appropriate

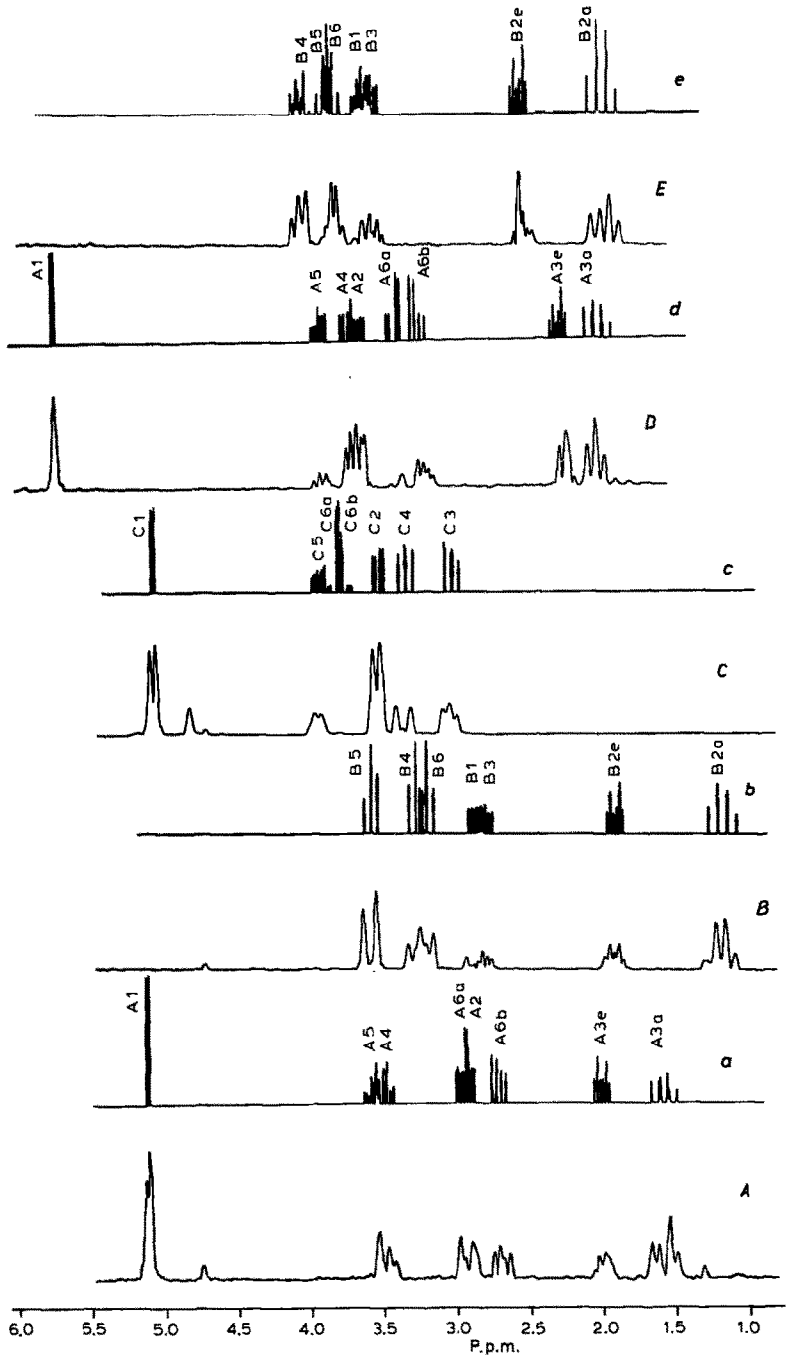

Fig. 5. Cross-sections extracted from 2D maps to represent "sub-spectra" appropriate to spin systems in rings A (*A*), B (*B*), and C (*C*) at pD 11.9 as well as in rings A (*D*) and B (*E*) at pD 3.9. Calculated sub-spectra are shown above each trace (*a–e*). Cross-section C was extracted from a homonuclear, ^{1}H triple-RCT experiment and all others were taken from the appropriate double-RCT maps at the sites indicated by heavy arrows in Figs. 3 and 6.

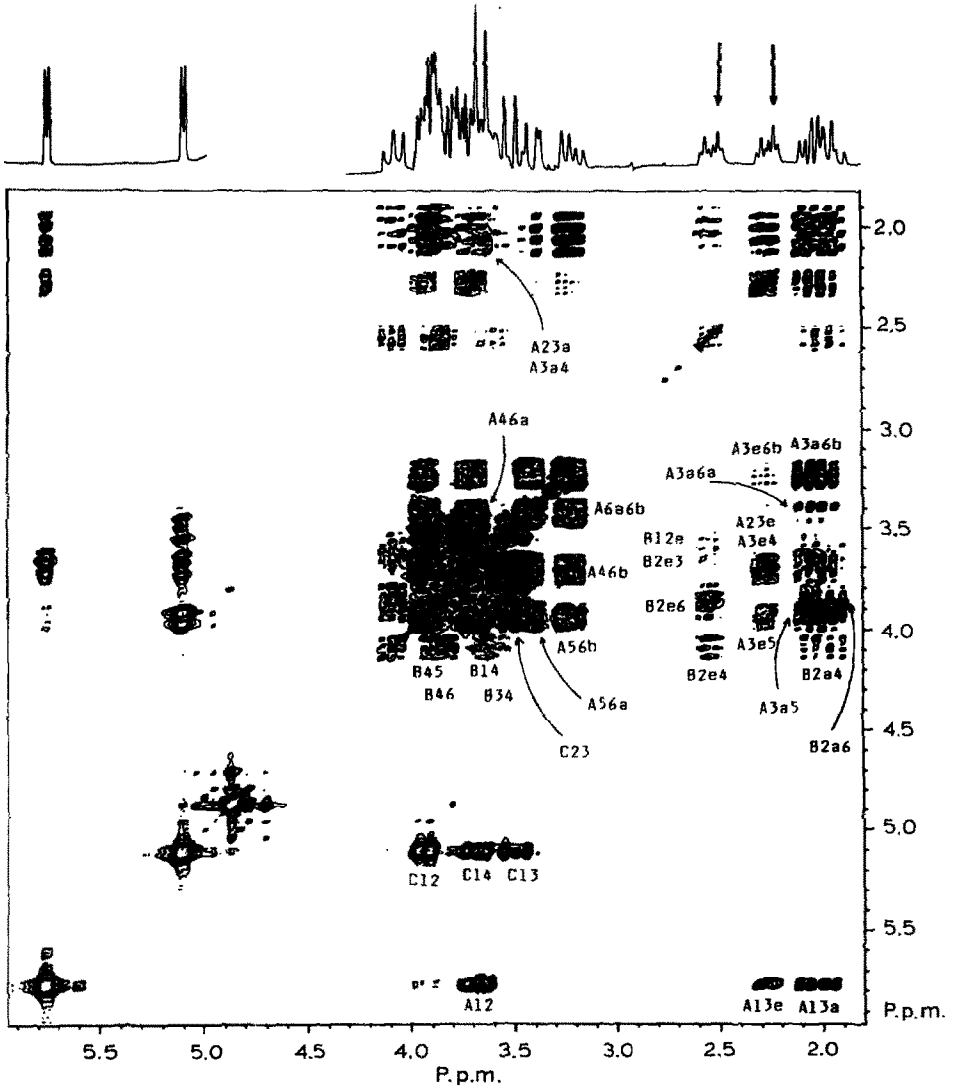

Fig. 6. Homonuclear, ^1H double-RCT 2D-map of tobramycin for a solution in D_2O at pD 3.9 and 40°. Other conditions are identical with those in the legend to Fig. 3. The heavy arrows point to sites at which vertical cross-sections *D* and *E* in Fig. 5 were taken.

2D map. Homonuclear 1D-n.O.e. measurements then allowed the two possible alternatives to be distinguished. Irradiation at the position of the doublet due to H-1′ resulted in a 12% enhancement in the intensity of a multiplet at 4.07 p.p.m. (in addition to a 13% increase in the intensity of the H-2′ multiplet; the "reverse" experiment, *i.e.*, irradiation at 4.07 p.p.m., caused the H-1′ doublet to increase in intensity by 14%). On the other hand, a rather complicated multiplet appeared at

~3.8 p.p.m. in the difference-n.O.e. spectrum on irradition at the position of the anomeric doublet at 5.12 p.p.m. (H-1″) (see Fig. 4D; an 18% n.O.e. was also observed, as expected, on the H-2″ multiplet at 3.95 p.p.m.). The splitting of the enhanced signal by 3.8 p.p.m. indicated that, in addition to the expected response from H-6, another proton contributed to the observed effect. This can only be H-5 (H-1 and H-3 being firmly assigned at ~3.6 p.p.m. from COSY correlations) and this effect is attributed to strong coupling between H-5 and H-6. This assumption was confirmed by spectrum simulation (see Fig. 4E). Another indication of the strong coupling between H-5 and H-6 is the appearance of "extra" lines in the multiplet due to H-4 at 4.07 p.p.m. ("virtual coupling"), which was reproduced well in the calculated spectrum (Figs. 1D and 4E). The relative chemical shifts for the resonances of H-1 and H-3 were finally determined from the DQ-COSY cross-multiplets 16 and 34, respectively (*cf.* the discussion of the data for pD 11.9). The "sub-spectrum" comprising the resonances of ring B, as extracted from the double-RCT map, is shown in Fig. 5.

Unlike the situation found at pD 11.9, the DQ-COSY experiment was of little assistance in deriving assignments for the kanosamine moiety (ring C) at pD 3.9. Owing to the quasi-coincidence of the resonances of H-5′, H-5, H-2″, and H-5″ (Table I), the corresponding cross-peaks all occurred in the same "row" of the COSY map and introduced uncertainty in the tracing of the *J*-connectivity path from, for example, H-2″ to H-3″. In contrast, various orders of RCT experiments, performed in succession, permitted unambiguous assignments to be deduced for resonances of ring C from H-1″ to H-5″ (Fig. 6), as for the spectrum recorded at pD 11.9. Since the expected cross-peaks 3″6″a and 3″6″b could not be identified with certainty in the double-RCT map (Fig. 6), the positions of the H-6″a and H-6″b resonances were anticipated on the assumption that protonation at a remote position (NH_2-3″) would have a negligible effect on the chemical shifts of the resonances H-6″a and H-6″b. The initial values thus obtained were then refined by spectrum simulation (*vide infra*).

The evidence supporting the assignment of the ^{1}H chemical shift data at each pD value is collected in Table I. Having thus established assignments for all non-exchangeable protons in the tobramycin molecule at both high and low pD values, the ^{1}H chemical shifts and *J* values were extracted from the resolution-enhanced 1D-n.m.r. spectra. These data were then used as input parameters for the PANIC spectrum-calculation program, and individual sub-spectra comprising the seven- or eight-spin systems for rings B, C, and A, respectively, were simulated. The spectral parameters (chemical shifts and *J* values) were then varied "manually" until a good visual fit to the experimental spectrum was attained. Co-addition of the calculated sub-spectra then yielded the composite spectra shown in Fig. 1. The ^{1}H chemical shifts and $J_{H,H}$ values resulting in the best-fit spectra are presented in Tables I and II.

The chemical shift data for the 2-deoxystreptamine (ring B) and kanosamine (ring C) residues are in excellent agreement with respective values for kanamycin

TABLE II

$J_{H,H}$ VALUES[a]

J	*pD 11.9*	*pD 3.9*
1′,2′	3.3	3.4
2′,3′*e*	4.4	4.4
2′,3′*a*	12.5	12.5
3′*e*,3′*a*	−12.0	−12.0
3′*e*,4′	4.4	4.3
3′*a*,4′	10.8	11.0
4′,5′	9.8	10.1
5′,6′a	2.6	3.8
5′,6′b	6.8	6.9
6′a,6′b	−13.7	−13.7
1,2*e*	4.2	4.2
1,2*a*	12.3	12.7
1,6′	9.4	9.4
2*e*,2*a*	−13.0	−12.8
2*e*,3	4.2	4.2
2*a*,3	12.2	12.8
3,4	9.5	10.5
4,5	9.5	8.4
5,6	9.4	10.0
1″,2″	3.9	3.7
2″,3″	10.4	10.7
3″,4″	9.4	10.3
4″,5″	10.0	10.4
5″,6″a	2.7	2.7
5″,6″b	4.3	4.8
6″a,6″b	−12.2	−12.2

[a]In Hz, measured for solutions in D_2O at 40°.

A (after allowance had been made for the different chemical-shift scale used) obtained[22] by application of "relative" methods of assignment. The agreement is very good also for the values of the protonation shifts, with notable exceptions for H-4 and H-4″ (the reported[22] $\Delta\delta_H$ values are 0.53 and 0.33 p.p.m., respectively). This difference may be indicative of minor conformational differences between kanamycin A and tobramycin in their protonated states due to the presence of an additional NH_2 group in tobramycin. Interactions of the protonated NH_2-3 with O-5′ in kanamycin A[23] and with the protonated NH_2-6′ in numerous other aminoglycoside antibiotics[4] have been invoked in rationalising ^1H and ^{13}C protonation shifts in terms of conformational changes associated with the protonation–deprotonation processes on changing the pH. However, the present example may indicate a possible role of interactions with the protonated NH_2-2′ in contributing to the conformational change undergone by the tobramycin molecule on protonation. In view of the well known difficulties encountered in rationalising ^1H protonation shifts in terms of structure and conformation[24], the limited data were not analysed further.

The $J_{H,H}$ values listed in Table II are consistent with those expected for essentially undistorted $^4C_1$ conformations in rings A–C. Similar values have been reported for the 2-deoxystreptamine[22,25] and kanosamine[22] moieties in neomycin B and kanamycin A, respectively. These values show up small differences in the two protonation states, which may be due to changes in the charge distribution on protonation and/or to small conformational distortions.

^{13}C-Assignments. — The ^{13}C-n.m.r. spectra of tobramycin and some related aminoglycoside antibiotics have been assigned[2], and similar data for numerous semi-synthetic derivatives have been reported[4]. All the assignments were based on comparisons with simpler model compounds and protonation shift data. It is desirable that such assignments be checked by the use of "absolute" techniques (such as 2D ^{1}H/^{13}C chemical-shift correlation, 1D or 2D INADEQUATE[26,27], *etc.*) whenever feasible. The ^{13}C assignments for tobramycin at low and high pD-values have been derived by a combination of 2D ^{1}H/^{13}C chemical-shift correlation[16] and 1D selective INEPT[17] techniques.

With all the ^{1}H chemical-shift data available, the 2D ^{1}H/^{13}C chemical-shift correlation experiment optimised to $^1J_{C,H}$ values constitutes the most straightforward method for assigning all but quaternary carbon resonances in a ^{13}C-n.m.r. spectrum. Ambiguities arise only for degenerate ^{1}H chemical shifts or strong coupling[28]. Although there are no exactly coincident ^{1}H chemical-shift values at pD 11.9 (Table I), some differences are small and care must be exercised in distinguishing ^{13}C resonances in correlation with near-coincident ^{1}H chemical shifts. These include the H-5/H-5′, H-4′/H-2″, H-4/H-4″, and H-1/H-3 pairs (differences in chemical shifts are 5.1, 4.6, 3.5, and 6.0 Hz, respectively). However by examining cross-sections parallel to the ^{1}H shift (F_1) axis extracted from the 2D map at the appropriate ^{13}C chemical shifts, differences as small as 2 Hz (0.01 p.p.m. at 200 MHz) could be distinguished in the ^{1}H shift (F_1) dimension. Thus, the choice between alternative assignments could be made with certainty except for the C-4/C-4″ pair; in this instance, the resonance of C-4 was assigned unambiguously on the basis of the "glycosylation shift"[29].

At pD 3.9, the smallest differences between ^{1}H chemical-shift values were all $\geq$0.02 p.p.m., so that ^{13}C assignments could be derived completely from the 2D ^{1}H/^{13}C correlation experiment optimised to $^1J_{C,H}$. However, further evidence was sought by the use of the selective INEPT[17] experiment. This allows the selective detection of ^{13}C resonances that have long-range scalar couplings ($^2J_{C,H}$ or $^3J_{C,H}$) to a proton in the molecule *via* magnetisation transfer from that proton to the ^{13}C nucleus. Application of this method to oligosaccharides provides a straightforward means, as demonstrated by Bax *et al.*[30], to determine the site of the glycosidic linkage *via* the $^3J_{C,H}$ coupling across the interglycosidic bond or, *vice versa*, to assign the resonances of ^{13}C nuclei, long-range coupled to the anomeric proton, in the ^{13}C-n.m.r. spectra of compounds with known structure. The latter approach was used here. Fig. 7 shows that application of a selective inversion pulse to the "inner" ^{13}C-satellite lines of H-1′ selectively enhanced the intensity of resonances already

assigned unambiguously to C-4 and C-3′ and of a third one at 70.36 p.p.m. In principle, the last resonance might be assigned either to C-2′ (due to transfer *via* $^2J_{C,H}$) or to C-5′ (magnetisation transfer *via* $^3J_{C,H}$). The former can be exluded beyond doubt both on chemical-shift arguments (a much lower chemical shift is to be expected for C-2′) and on the expected[30] low $^2J_{C\text{-}2',H\text{-}1'}$ value. The assignment for C-5′ accords with that deduced above from the $^1H/^{13}C$ chemical-shift correlation and with literature data[2]. The "complementary" experiment, *i.e.*, selective inversion of the inner satellite lines belonging to H-1″, corroborated the assignments for C-3″, C-5″, and C-6 (Fig. 7). A further argument in favour of assigning the resonance at 72.93 p.p.m. to C-5″ (as opposed to C-2″) is the low value of the protonation shift in contrast to that expected[2] for a carbon (such as C-2″) in a position β to a protonatable group. Another group of ^{13}C resonances with similar ^1H chemical shifts include C-4′, C-4″, and C-2′. Of these, C-2′ has already been firmly assigned above, whereas C-4″ can be identified simply by considering protonation shifts (Table III), which are 4.29 p.p.m. for C-4″ (β "upfield" shift[2]) and only 1.82 p.p.m. for C-4′. This result accords with the assignment obtained from the $^1H/^{13}C$ chemical-shift correlation experiment.

When these assignments and protonation shift data (Table III) are compared with those obtained[2] by "relative" methods, it can be stated that the latter are essentially correct apart from minor uncertainties affecting, especially, C-1, C-3, and C-2′, each of which is linked to an amino group. However, the two sets of chemical-shift values (Table III) show quantitative differences of up to ~1 p.p.m.

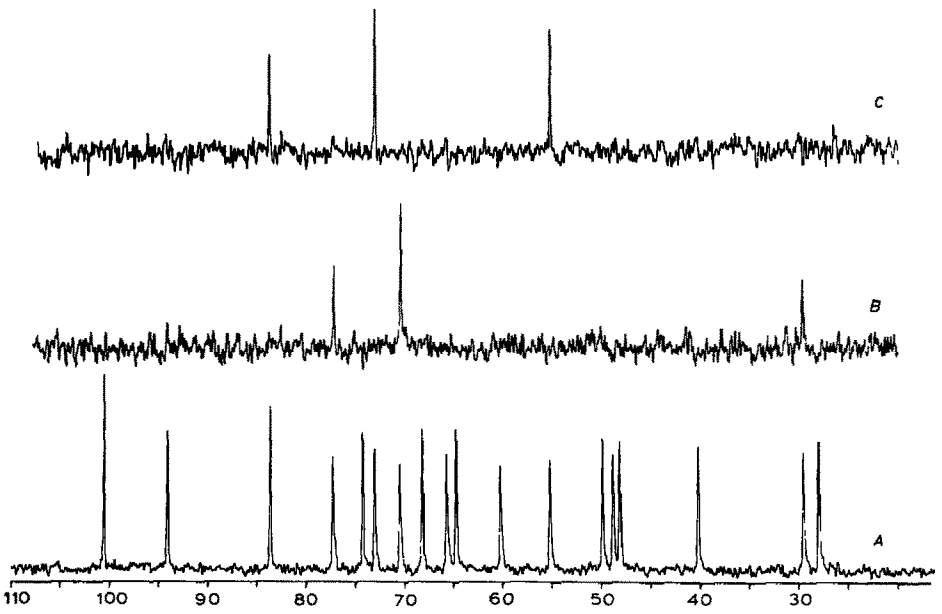

Fig. 7. ^{13}C-N.m.r. spectrum of a solution of tobramycin in D_2O, at pD 3.9 and 40° (*A*), together with selective INEPT spectra obtained by applying selective inversion pulses to H-1′ (*B*) or H-1″ (*C*).

TABLE III

^{13}C-N.M.R. DATA[a] (50 MHz)

Carbon atom	*Chemical shift*[b]		*Protonation shift*[c]
	pD 11.9	*pD 3.9*	
1′	99.99 (0.79)	94.03	5.96 (5.9)
2′	49.38 (0.39)	47.94	1.45 (1.6)
3′	35.25 (0.55)	29.35	5.90 (5.5)
4′	66.48 (0.58)	64.66	1.82 (1.4)
5′	74.16 (1.06)	70.36	3.80 (3.1)
6′	41.94 (0.44)	41.07	0.87 (0.7)
1	50.46 (0.26)	49.74	0.72 (0.6)
2	35.94 (0.44)	27.82	8.12 (7.8)
3	49.67 (0.17)	48.58	1.09 (1.3)
4	86.95 (0.95)	77.20	9.75 (9.2)
5	74.70 (0.30)	74.22	0.48 (0.5)
6	88.40 (0.60)	83.61	4.79 (4.5)
1″	100.04 (0.94)	100.57	−0.51 (−1.0)
2″	72.17 (0.57)	68.10	4.07 (3.7)
3″	54.57 (0.37)	55.01	−0.44 (−0.7)
4″	69.82 (0.62)	65.53	4.29 (3.9)
5″	72.53 (0.63)	72.93	−0.40 (−0.6)
6″	60.79 (0.59)	60.04	0.75 (0.4)

[a]External Me_4Si for solutions in D_2O at 40°. [b]Values given in parentheses: δ (this work) − δ (ref. 2). [c]δ (pD 11.9) − δ (pD 3.9); values in parentheses are those given in ref. 2.

at each carbon; the largest differences are observed for carbons β to amino groups, which reflect differences in the extents of protonation. Other factors that may contribute to the differences observed are sample concentration and temperature (not reported in ref. 2; we have observed temperature shifts of 0.11–0.18 p.p.m./10° for the resonances of C-2, C-4, C-2″, C-4″, and C-6″). In agreement with others[4], considerable variations in ^{13}C chemical shifts upon exposure of the sample at pD 11.9 to even relatively small amounts of CO_2 have been found. For compounds susceptible to protonation in general, and for aminoglycoside antibiotics in particular, it is important to conduct measurements under rigorously defined conditions.

EXPERIMENTAL

Tobramycin free-base, obtained from the Biogal Pharmaceutical Works (Debrecen, Hungary), in 0.1M solutions in D_2O was used for both ^{1}H- and ^{13}C-n.m.r. measurements. The D_2O and the samples were purged thoroughly with dry argon and all subsequent manipulations were performed under argon. M Solutions of NaOD and DCl in D_2O were used for adjusting the pD, and exact pD values were determined directly in the 5-mm n.m.r. tubes using a pH meter equipped with a combination microelectrode (Ingold Electrodes, Inc., No. 6030-02). The values are given as direct meter readings.

The ^1H chemical shifts are referenced to internal sodium 4,4-dimethyl-4-silapentane-1-sulfonate and external Me_4Si was used for the ^{13}C chemical shifts. 200-MHz ^1H- and 50-MHz ^{13}C-n.m.r. spectra were recorded with a Bruker WP 200 SY spectrometer. All measurements were carried out at 40 ±1°, using the BVT-1000 variable-temperature unit.

The pure-phase DQ-COSY experiments were carried out by the TPPI procedure[12] with the aid of a standard microprogram of the Bruker software DISNMR/P, version 860101.1. The residual HDO signal was suppressed by low-power (DP setting 45L) pre-irradiation during 1.5 s in the "homo-gated" mode prior to the first pulse of the DQ-COSY pulse sequence. The 2D $^1H/^{13}C$ chemical-shift correlation maps were produced with the aid of a pulse sequence[16] devised to eliminate $^1H/^1H$-couplings, and adequate digital resolution in the F_1 dimension was ensured (1.08 Hz/point) in order to determine the ^1H frequency differences using cross-sections parallel to the F_1 (^1H) frequency axis of the 2D map. The selective INEPT[17] measurements were performed with the aid of a microprogram written in analogy with the standard refocused INEPT[31], $\pi/2(H)–\Delta_1/2–\pi(H)\pi(C)–\Delta_1/2–\pi/2(H)\pi/2(C)–\Delta_2/2–\pi(H)\pi(C)–\Delta_2/2–^{13}C$ acquisition with BB decoupling. In the above pulse sequence, all proton pulses are selective (soft) pulses [$\tau(\pi/2)$ ~13 ms] and $\Delta_1 = (2J)^{-1} - 3\,\tau(\pi/2)$, $\Delta_2 = (2J)^{-1} - 2\tau(\pi/2)$. In calculating the Δ_1 and Δ_2 values, an estimated long-range $J_{C,H}$ value of 5 Hz was used. The phase program was adopted from the basic non-selective INEPT experiment (standard Bruker microprogram, INEPTRD.AU). The different RCT experiments were executed with microprograms closely following the published procedure[14]. Listings are available upon request. Relevant experimental details are given with the caption to Fig. 3. The 1D-homonuclear n.O.e. measurements were executed in the difference mode[15], using frequency cycling[32] and a composite 90° readout-pulse to minimise population transfer effects[33]. For saturation of selected multiplets, one-hundred 0.1-s decoupler pulses (power level setting, 50L) were used under frequency cycling amounting to a total pre-irradiation time of 10 s.

ACKNOWLEDGMENT

Financial support from the Hungarian Academy of Sciences (grant no. OTKA-274/86) is gratefully acknowledged.

REFERENCES

1 J. Bérdy, A. Aszalos, M. Bostian, and K. L. McNitt, *CRC Handbook of Antibiotic Compounds*, Vol. I, CRC Press, Boca Raton, Florida, 1980, pp. 85–245.
2 K. F. Koch, J. A. Rhoades, E. W. Hagaman, and E. Wenkert, *J. Am. Chem. Soc.*, 96 (1974) 3300–3305.
3 F. Le Goffic, J. F. Le Bigot, S. Sicsic, and C. Vincent, *Nouv. J. Chim.*, 4 (1980) 53–57.
4 P. J. L. Daniels, A. K. Mallams, S. W. McCombie, J. B. Morton, T. L. Nagabhushan, D. F. Rane, P. Reichert, and J. J. Wright, *J. Chem. Soc., Perkin Trans. 1*, (1981) 2209–2227.
5 D. E. Dorman, J. W. Paschal, and K. E. Merkel, *J. Am. Chem. Soc.*, 98 (1976) 6885–6888.
6 L. Szilágyi, *Carbohydr. Res.*, 118 (1983) 269–275.

7 A. BAX AND R. FREEMAN, *J. Magn. Reson.*, 44 (1981) 542–561.
8 J. N. SCARSDALE, J. H. PRESTEGARD, S. ANDO, T. HORI, AND R. K. YU, *Carbohydr. Res.*, 155 (1986) 45–56.
9 J. FEENEY, T. A. FRENKIEL, AND E. F. HOUNSELL, *Carbohydr. Res.*, 152 (1986) 63–72.
10 D. R. BUNDLE, M. GERKEN, AND M. B. PERRY, *Can. J. Chem.*, 64 (1986) 255–264.
11 U. PIANTINI, O. W. SØRENSEN, AND R. R. ERNST, *J. Am. Chem. Soc.*, 104 (1982) 6800–6801; M. RANCE, O. W. SØRENSEN, G. BODENHAUSEN, G. WAGNER, R. R. ERNST, AND K. WÜTHRICH, *Biochem. Biophys. Res. Commun.*, 117 (1983) 479–485.
12 D. MARION AND K. WÜTHRICH, *Biochem. Biophys. Res. Commun.*, 113 (1983) 967–974.
13 G. EICH, G. BODENHAUSEN, AND R. R. ERNST, *J. Am. Chem. Soc.*, 104 (1982) 3732–3733.
14 A. BAX AND G. DROBNY, *J. Magn. Reson.*, 61 (1985) 306–320.
15 L. D. HALL AND J. K. M. SAUNDERS, *J. Am. Chem. Soc.*, 102 (1980) 5703–5711.
16 A. BAX, *J. Magn. Reson.*, 53 (1983) 517–520; V. RUTAR, *ibid.*, 58 (1984) 306–310; J. A. WILDE AND P. H. BOLTON, *ibid.*, 59 (1984) 343–346.
17 A. BAX, *J. Magn. Reson.*, 57 (1984) 314–318.
18 R. J. ABRAHAM, *The Analysis of High Resolution NMR Spectra*, 1st edn., Elsevier, Amsterdam, 1971, pp. 72–74.
19 J. DĄBROWSKI, P. HANFLAND, H. EGGE, AND U. DĄBROWSKI, *Arch. Biochem. Biophys.*, 210 (1981) 405–411.
20 M. A. BERNSTEIN AND L. D. HALL, *J. Am. Chem. Soc.*, 104 (1982) 5553–5555.
21 T. A. W. KOERNER, JR., J. N. SCARSDALE, J. H. PRESTEGARD, AND R. K. YU, *J. Carbohydr. Chem.*, 3 (1984) 565–580.
22 K. BOCK, *Annu. Rep. NMR Spectosc.*, 13 (1982) 15–16.
23 R. U. LEMIEUX, T. L. NAGABHUSHAN, K. J. CLEMETSON, AND L. C. N. TUCKER, *Can. J. Chem.*, 51 (1973) 53–66.
24 O. JARDETZKY AND G. C. K. ROBERTS, *NMR in Molecular Biology*, 1st edn., Academic Press, New York, 1981, pp. 34–37.
25 R. E. BOTTO AND B. COXON, *J. Carbohydr. Chem.*, 3 (1984) 545–563.
26 A. BAX, R. FREEMAN, AND T. A. FRENKIEL, *J. Am. Chem. Soc.*, 103 (1981) 2102–2103.
27 T. A. MARECI AND R. FREEMAN, *J. Magn. Reson.*, 48 (1982) 158–163.
28 G. A. MORRIS AND K. I. SMITH, *J. Magn. Reson.*, 65 (1985) 506–509.
29 R. KASAI, M. SUZUO, J. ASAKAWA, AND O. TANAKA, *Tetrahedron Lett.*, (1977) 175–178; K. TORI, S. SEO, Y. YOSHIMURA, H. ARITA, AND Y. TOMITA, *ibid.*, (1977) 179–182.
30 N. CYR, G. K. HAMER, AND A. S. PERLIN, *Can. J. Chem.*, 56 (1978) 297–301; A. BAX, W. EGAN, AND P. KOVAČ, *J. Carbohydr. Chem.*, 3 (1984) 593–611.
31 D. P. BURUM AND R. R. ERNST, *J. Magn. Reson.*, 39 (1982) 163–168.
32 M. KINNS AND J. K. M. SANDERS, *J. Magn. Reson.*, 56 (1984) 518–520; K. E. KÖVÉR, *ibid.*, 59 (1984) 485–488.
33 A. J. SHAKA, C. BAUER, AND R. FREEMAN, *J. Magn. Reson.*, 60 (1984) 479–485.